ISSN 1023-1935, Russian Journal of Electrochemistry, 2018, Vol. 54, No. 3, pp. 292–301. © Pleiades Publishing, Ltd., 2018.
Published in Russian in Elektrokhimiya, 2018, Vol. 54, No. 3, pp. 337–348.

Highly Sensitive Nanostructured Electrochemical Sensor Based on Carbon Nanotubes-Pt Nanoparticles Paste Electrode for Simultaneous Determination of Levodopa and Tyramine[1]

Mehdi Baghayeri[a], *, Hadi Beitollahi[b], Ali Akbari[c], and Samaneh Farhadi[a]

[a] *Department of Chemistry, Faculty of Science, Hakim Sabzevari University, P.O. Box 397, Sabzevar, Iran*
[b] *Environment Department, Institute of Science and High Technology and Environmental Sciences, Graduate University of Advanced Technology, Kerman, Iran*
[c] *Department of Chemistry, University of Jiroft, Jiroft, Iran*
**e-mail: mehdi.baghayeri@yahoo.com*

Received May 21, 2016; in final form, October 4, 2016

Abstract—A multicomponent electrochemical sensor, with two nanometer-scale components in sensing matrix/electrode, was used to simultaneous determination of levodopa (LD) and tyramine (TR) in pharmaceutical and diet samples. Multiwall carbon nanotubes (MWCNTs) were used as carbonaceous materials in the electrode construction. 5-amino-3',4'-dimethoxy-biphenyl-2-ol (5ADMB) was used as electron mediator and Pt nanoparticles (nPt) as a catalyst. The 5ADMB catalyzes the oxidation of LD to the corresponding catecholamine, which is electrochemically reduced back to LD. Preparation of this electrode was very simple and modified electrode showed good properties at electrocatalytic oxidization of LD and TR. Using differential pulse voltammetry (DPV), a highly selective and simultaneous determination of LD and TR has been explored at the modified electrode. Differential pulse voltammetry peak currents of LD and TR increased linearly with their concentrations at the ranges of 0.50–100.0 μM and 0.60–100.0 μM, respectively. Also, the detection limits for LD and TR were 0.31 and 0.52 μM, respectively. The electrode exhibited an efficient catalytic response with good reproducibility and stability.

Keywords: Pt nanoparticles, catalysis, tyramine, levodopa, multi-walled carbon nanotube
DOI: 10.1134/S1023193517120023

INTRODUCTION

Tyramine (1-hydroxy-4-ethylaminobenzene; TR) produced by the decarboxylation of amino acid tyrosine, is one of the biogenic amines, which were produced as degradation products resulting from the microbial activity. It is found commonly in fermented foods and beverages, meat, fish, seafood and dairy products [1–3]. It has been reported that tyramine containing foods can cause unnatural and toxic effects, when ingested in large quantities [4]. Therefore development of a fast and accurate method to measure tyramine concentrations in foods would be important. Many techniques have been developed and improved for detection and quantification of tyramine in different food products, including fluorimetry [5], thin layer chromatography and spectrofluorometry [6], capillary electrophoresis [7], quantitative PCR [8] and high-performance liquid chromatography (HPLC) with fluorimetric detection and electrochemical detection, has been applied for tyramine determinations [9, 10]. However, these methods require extensive sample pretreatments and expensive equipment. Electrochemical determination of tyramine using chemically modified electrodes has been reported in the literature, as a good and cheap alternative to the traditional methods [11, 12].

The unusual amino acid levodopa (3,4-dihydroxyphenylalanine, LD) is the precursor required by the brain to produce dopamine, a neurotransmitter (chemical messenger in the nervous system). People with Parkinson's disease have depleted levels of dopamine and levodopa is used to increase dopamine in the brain, which reduces the symptoms of Parkinson's disease [13]. Therefore, the determination of LD has attracted much attention of researchers. Among the various methods available for determination of LD such as HPLC [14] and capillary zone electrophoresis [15], electrochemical detections are rapid, economic, highly sensitive and specific [16, 17].

Cheese and yeast products are potentially dangerous in individuals being treated with monoamine oxidase (MAO) inhibitors because consumption of these products could provide the 10 mg of tyramine needed to cause a severe hypertensive crisis [18]. Inhibition of

[1] The article is published in the original.

MAO by MAO inhibitors allows tyramine to avoid metabolic degradation and provides for the release of catecholamines present in elevated amounts at nerve endings, the adrenal medulla, and other peripheral sites [19]. On the other hand, LD can also cause hypertensive crisis when MAO is inhibited. Therefore, patients receiving nonspecific MAO inhibitor medications must restrict tyramine in the diet and cannot take levodopa [20]. Therefore, their simultaneous determination of LD and TR is quite necessary for treatment of diseases.

Modified electrodes based on the incorporation of mediators and nanoparticles within carbon paste are gaining considerable attention. Even though his recent research project does not involve carbon paste electrode, this unique electrode has found its way back into many researchers laboratory in the past decade, especially in the area of biosensor research. Short response times accrue from the absence of supporting membranes and the close proximity of the catalyst and graphite sites. The bulk of the paste serves as a source of the catalytic activity, and fresh surfaces can easily be obtained by renewing the surface [21]. In recent years, nanomaterials, such as carbon nanotubes (CNTs) and metal nanoparticles (NPs), have been widely applied to the fabrication of biosensors with the aim to improve the property of biosensors. CNTs have many unique properties [22–27], and they can promote the electron-transfer of a wide range of electroactive species. This is favorable to enhancing the characteristic of sensors. Metal nanoparticles generally have high effective surface area, catalysis and biocompatibility [28, 29]. Among various metallic NPs, platinum NP is very important. Many studies focus on its application as a catalyst in electrochemistry [30, 31], immobilization of enzymes [32] and so on.

In a previous work, we demonstrated the sensitive detection of acetaminophen and phenobarbital using a composite matrix that combines the electrocatalytic activity of Pt nanoparticles and multi-walled carbon nanotubes (MWCNTs) into a simple paste [33]. In this article, we present results for a new electrochemical sensor, which consists of 5-amino-3',4'-dimethoxy-biphenyl-2-ol (5ADMB) as an electron transfer mediator, for the sensitive determination of LD in presence of TR and its application in measuring of these two important biological compounds in the in real samples.

EXPERIMENTAL

Apparatus and Chemicals

Electrochemical experiments were carried out using a computerized potentiostat/galvanostat (Autolab model 302 N, Eco Chemie B.V.A). The experimental conditions were controlled with General Purpose Electrochemical System (GPES) software. A conventional three-electrode cell was used at 25 ± 1°C. An Ag|AgCl|KCl (3.0 M) electrode, a platinum wire, and an nPt-5ADMBCNPE were used as the reference, auxiliary and working electrodes, respectively. A Metrohm 691 pH/ion meter was also used for pH measurements. All solutions were freshly prepared with twice distilled water. LD, TR and reagents were analytical grades from Sigma. 5ADMB and CNTs (the diameter, length, purity and surface area of CNTs was ~2.5 nm (outer diameter of CNTs is in the range of 1.52–3.54 nm), 5–15 μm, 90%, 97 m^2/g (roughly), respectively) were synthesized in our laboratory as reported previously [34]. High viscosity paraffin (density = 0.88 g cm^{-3}) from Fluka was used as the pasting liquid. Phosphate buffered solutions (PBS) 0.1 M for different pH values were prepared by mixing stock solutions of 0.1 M H_3PO_4, NaH_2PO_4, Na_2HPO_4 and Na_3PO_4. Potassium chloride from Fluka was used as the supporting electrolyte. A Philips model XL30 scanning electron microscope (SEM) was used to determine the morphology of the synthesized Pt-nanoparticles sample. The biological samples used in this work were obtained from Medical Diagnostic Laboratory, Sabzevar, Iran. All other used reagents were of analytical grade.

Preparation of Pt-Nanoparticles

The Pt nanoparticles were obtained by reducing hexachloroplatinate to metallic Pt with sodium borohydride in aqueous solution, as reported at our previous literature [33]. For this purpose, H_2PtCl_6 (3.38 mM) was dissolved in 50 mL of doubly distilled water and an excess amount of $NaBH_4$ was then added to the H_2PtCl_6 solution under stirring. After 2 h, the Pt nanoparticles were separated from the reaction mixture and washed with double distilled water three times. Finally, the purified Pt nanoparticles were dried without any heat treatment. The resulting Pt nanoparticles were grind and kept at 4°C before using in the surface modification of electrodes. The morphology and nanostructure distribution of the Pt nanoparticles were recorded by SEM (Fig. 1).

Preparation of the Electrodes

Carbon nanotube paste electrodes were prepared by hand mixing 0.01 g 5ADMB with 85-times its weight of graphite powder, 4-times its weight of Pt nanoparticles and 10-times its weight of carbon nanotube with a mortar and pestle. Paraffin was added to the above mixture using a 5 mL syringe and mixed for 20 min until a uniformly wetted paste was obtained. The paste was then packed into the end of a glass tube (ca. 2 mm i.d. and 10 cm long). A copper wire inserted into the carbon paste provided the electrical contact. When necessary, a new surface was obtained by pushing an excess of paste out of the tube and then polished with a weighing paper. The unmodified electrodes

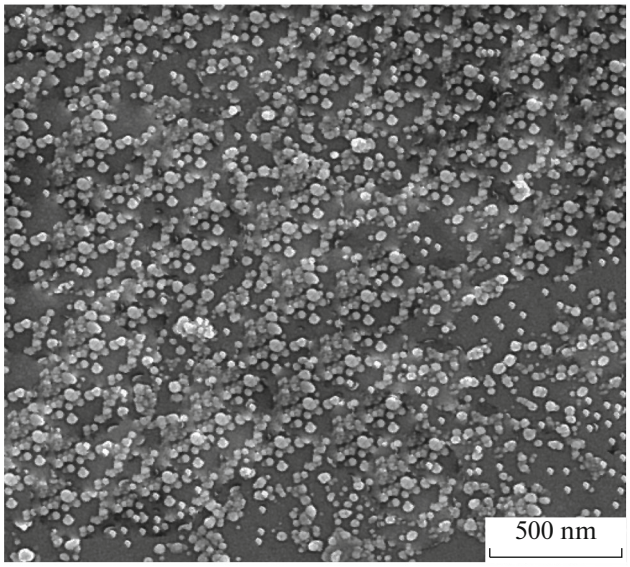

Fig. 1. Scanning electron micrographs of Pt nanoparticles spread on a carbon paper.

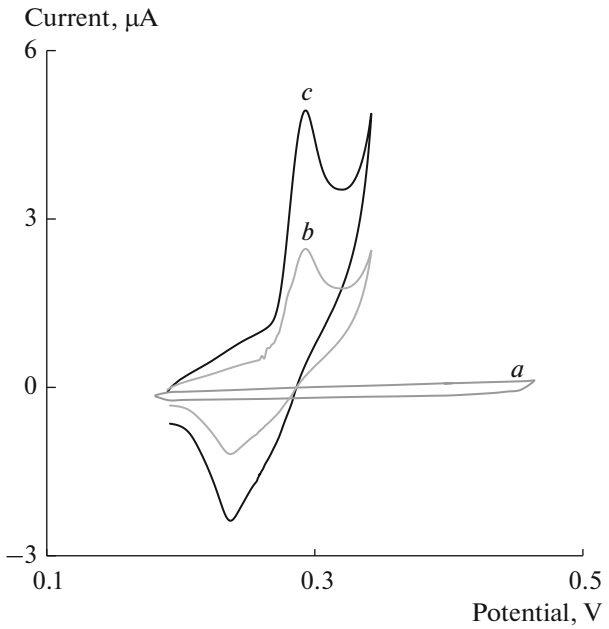

Fig. 2. Cyclic voltammograms of (*a*) nPt-CNPE, (*b*) 5ADMBCNPE and (*c*) nPt-5ADMBCNPE in a 0.1 M PBS (pH 7.0) at the scan rates of 20 mV s^{-1}.

were prepared in the same way without adding Pt nanoparticles (5ADMBCNPE), MWCNTs (nPt-5ADMBPE), 5ADMB (nPt-CNPE) and using only graphite powder (CPE).

Preparation of Real Samples

1.0 mL yoghurt was first mixed with 5 mL anhydrous alcohol. After 10 min sonication and 5 min shaking, the mixture was centrifuged for 10 min, and then the supernatant was filtrated. The filtrate was collected and added into 25 mL volumetric flask, diluted with twice distilled water to the marked line.

A solution of 0.1 M NaOH was added to the urine solution. The mixture was vortexed for 3 min after which 3 mL ethyl acetate was added and the mixture was vortexed for an additional 3 min. The mixture was centrifuged at 3000 rpm for 10 min to separate the aqueous and organic layers. The residual aqueous phase was reconstituted with 0.1 M PBS at pH 7.0 and used for analytical determinations.

RESULTS AND DISCUSSION

Electrochemical Behavior of nPt-5ADMBCNPE

Cyclic voltammetry (CV) technique was applied to investigate the electrochemical behavior of different electrodes during the fabrication process. Figure 2 presents the CVs of nPt-CNPE, 5ADMBCNPE and nPt-5ADMBCNPE in PBS (0.1 M, pH 7.0). As shown in Fig. 2, no redox peak was observed for nPt-CNPE in the potential range from 0.18 up to 0.46 V (Fig. 2a). As shown in Fig. 2c, in the presence of Pt nanoparticles in the electrode, a reversible redox couple with formal potential of 0.29 V (Ag|AgCl|KCl (3.0 M)) and peak height of 4.92 μA is observed, indicating the presence of $5ADMB_{ox}/5ADMB_{red}$ redox couple. It is clear that the peak to peak separation of $5ADMB_{ox}/5ADMB_{red}$ redox couple is about 50 mV at scan rate 20 mV s^{-1} at nPt-5ADMBCNPE, suggesting facile charge transfer kinetic of mediator in the presence of Pt nanoparticles [34]. The electrode capability for the generation of a reproducible surface was examined by cyclic voltammetric data obtained in optimum solution pH 7.0 from seven separately prepared modified electrodes. The calculated RSD for various parameters accepted as the criteria for a satisfactory surface reproducibility (about 2.4%), which is virtually the same as that expected for the renewal or ordinary carbon paste surface [35]. However, we regenerated the surface of modified electrode before each experiment. We calculated the heterogeneous electron transfer rate constant (k_s) of 5ADMB incorporated into electrode from the dependence of peak-to-peak separation (ΔE_p) on the various scan rates, according to the Laviron model [36]. Taking a charge transfer coefficient (α) of 0.5, then the electron transfer rate constant (k_s) was 9.62 ± 0.1 s^{-1}. This value is higher than reported value of (k_s) for modified electrode in absence of Pt nanoparticles, 7.94 s^{-1} [37]. Therefore, Pt nanoparticles can facilitate the electron transfer reaction. This can be as a result of the strong interaction between 5ADMB molecules and Pt nanoparticles. It is proposed that the presence of nanoparticles increase the effective surface area and active point for interaction catalyst (here 5ADMB) and graphite sites.

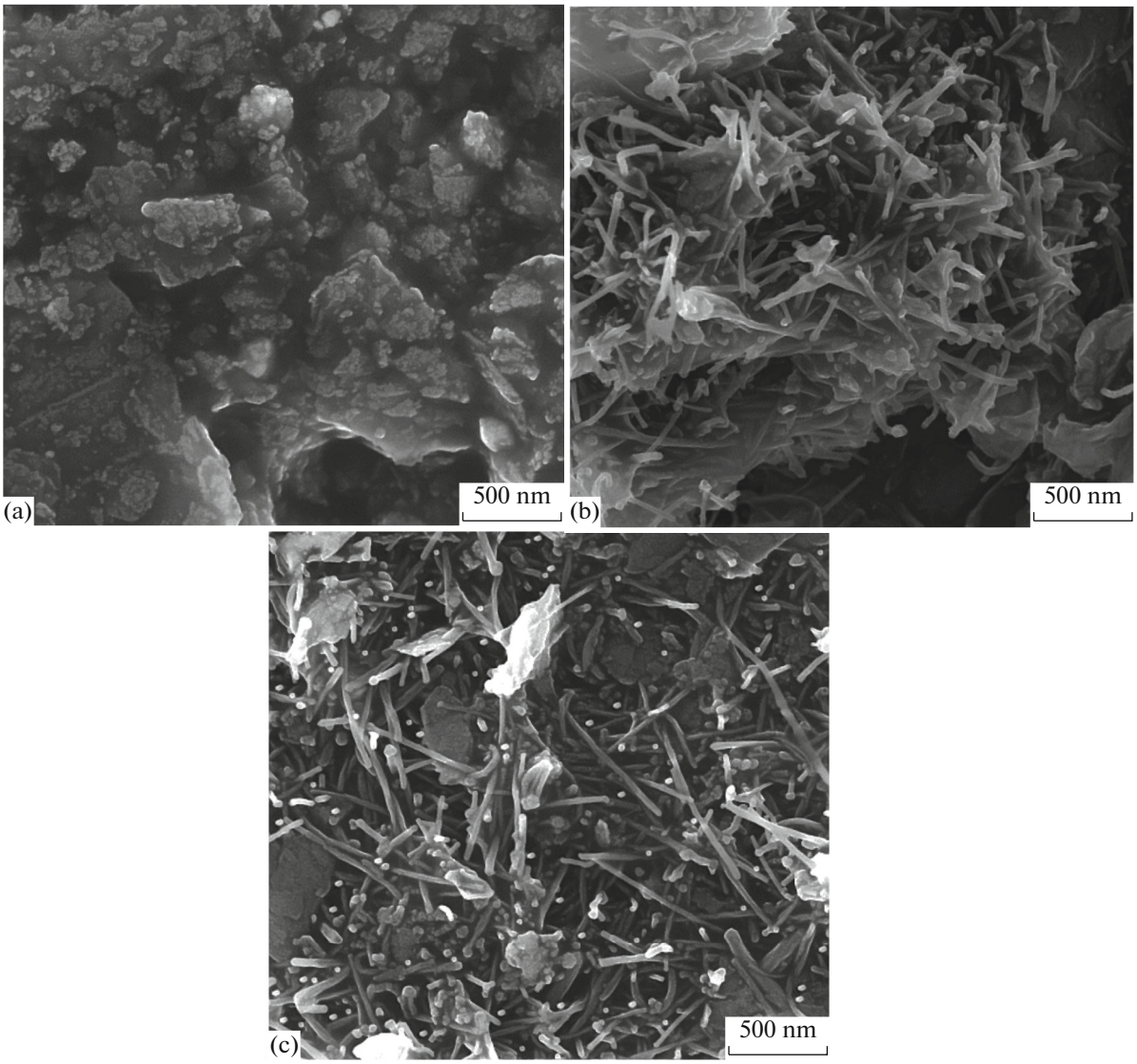

Fig. 3. SEM images of (a) CPE, (b) MWCNT/CPE and (c) nPt-5ADMBCNPE.

They also make the surface more porous for facilitating electron transfer.

The stability of modified electrode was checked by repetitive cycling at scan rate of 20 mV s^{-1}. In the first 5 scans, the anodic and cathodic currents decreased with scan number, but the currents then remained at 91–94% of the initial value after 45 cycles. Further, three different electrodes: CPE, CNPE and nPt-CNPE have been prepared with similar conditions and have been characterized using SEM. Figure 3a indicates the morphology of CPE surface after polishing. As shown in this image, there are some defects on the electrode surface that obtained during polishing the surface of electrode. Figure 3b shows the SEM image of the surface of the electrode when MWCNTs are added for construction of the electrode. The electrode surface in Fig. 3b is relatively porous despite the presence of some rough regions. The SEM of nPt-5ADMBCNPE shows that Pt nanoparticles were regularly dispersed in electrode surface exhibiting uniform porous structure (Fig. 3c). This structure could provide a significant increase of effective electrode surface. The significant roughness and high porosity observed in Fig. 3c seems to have considerable influence on the accessible active areas and increase of effective electrode surface.

Electrocatalytic Oxidation of LD on nPt-5ADMBCNPE

Due to stability, electrochemical reversibility and high electron transfer rate constant of $5ADMB_{ox}/5ADMB_{red}$ redox couple at nPt-5ADMBCNPE, it can be used as a good mediator to shuttle electrons between electrode and analytes. In order to test the electrocatalytic abil-

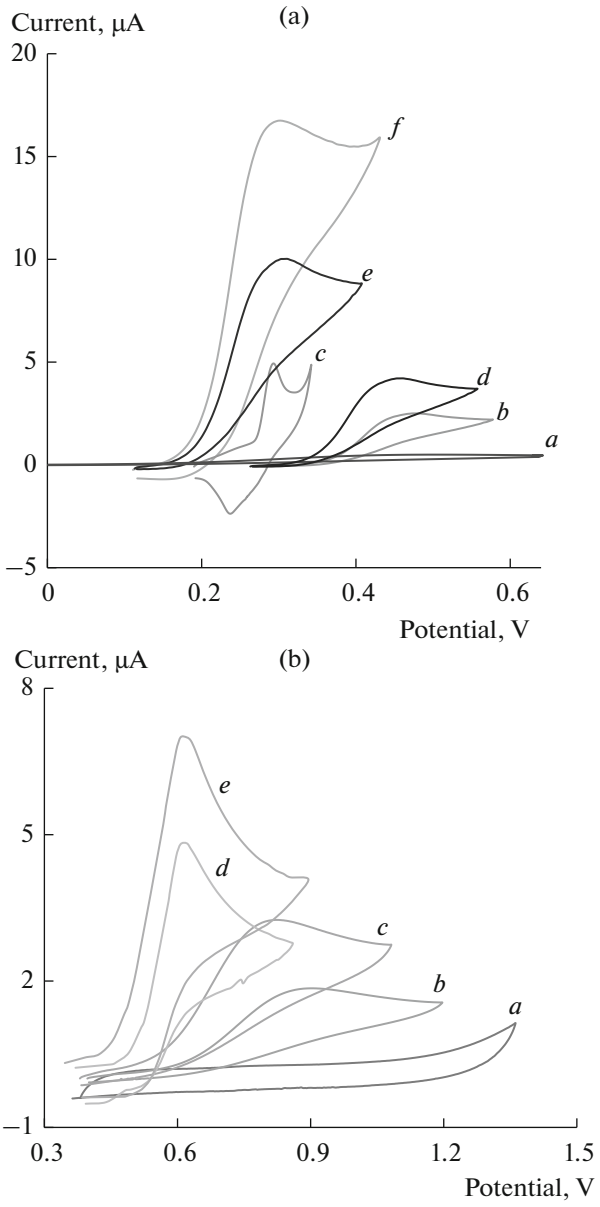

Fig. 4. (a) Cyclic voltammograms (*a*) in the absence and (*b*) presence of 80.0 μM LD in 0.1 M PBS (pH 7.0) at the surface of CPE at scan rate 20 mV s^{-1}. (*c*) as (*a*) and (*d*) as (*b*) at the surface of nPt-5ADMBCNPE and nPt-CNPE, respectively. Also (*e*) and (*f*) as (*b*) at the surface of 5ADMBCNPE and nPt-5ADMBCNPE, respectively. (b) Cyclic voltammogram of CPE in the absence of TR (*a*) and cyclic voltammograms of 40.0 μM TR in 0.1 M PBS (pH 7.0) recorded at different electrodes CPE (*b*), 5ADMBCNPE (*c*), nPt-CNPE (*d*) and nPt-5ADMBCNPE (*e*). Scan rate: 20 mV s^{-1}.

ity of this modified electrode, cyclic voltammograms of modified and unmodified electrodes were recorded in the absence and presence of LD and TR.

Figure 4a depicts the cyclic voltammetric responses from the electrochemical oxidation of 80.0 μM LD at nPt-5ADMBCNPE (curve *f*), 5ADMBCNPE (curve *e*), nPt-CNPE (curve *d*), bare CPE (curve *b*). As can be seen, the anodic peak potential for the oxidation of LD at nPt-5ADMBCNPE (curve *f*) and 5ADMBCNPE (curve *e*) is about 0.29 V, while at the nPt-CNPE (curve *d*) peak potential is about 0.44 V, and at the bare CPE peak potential is about 0.47 V for LD (curve *b*). From these results, it is concluded that the best electrocatalytic effect for LD oxidation is observed at nPt-5ADMBCNPE (curve *f*). As it can be seen, the oxidation peak potential of LD at nPt-5ADMBCNPE (curve *f*) is shifted about 0.14 and 0.17 mV toward less positive potential compared with that at nPt-CNPE (curve *d*) and bare CPE (curve *b*), respectively. Similarly, when we compared the oxidation of LD at the nPt-5ADMBCNPE (curve *f*) and 5ADMBCNPE (curve *e*), there was an abundant enhancement on the electrocatalytic oxidation peak current at nPt-5ADMBCNPE versus the value obtained at the 5ADMBCNPE. In the other words, the data obtained clearly show that the addition of Pt nanoparticles to electrode substrate definitely improves the electrocatalytic oxidation of LD.

Also, cyclic voltammograms of 40 μM TR in 0.1 M PBS (pH 7.0) on different electrodes were recorded with the results shown in Fig. 4b. At mentioned four electrodes, only one oxidation peak was observed from +0.3 to +1.4 V, showing that TR suffered an irreversible redox process. The oxidation of TR at CPE occurred at the potential of 0.88 V with poor current response (I_p = 1.64 μA) (curve *b*), indicating a slow electron transfer kinetic. For 5ADMBCNPE, the peak current of TR was larger than that obtained at CPE (I_p = 3.15 μA). What is more, the peak shapes were well-defined and the peak potentials shifted negatively to 0.80 V (curve *c*). These phenomena suggest that the oxidation of TR is more favorable at the 5ADMBCNPE, which is undoubtedly attributed to the unique characteristics of modified electrode as excellent electric conductivity, high surface area. At nPt-CNPE, the oxidation potential shifted positively to 0.60 V (curve *d*), and the peak current (I_p = 4.8 μA) suggested the faster electron transfer due to the high conductivity of nPt. While on the nPt-5ADMBCNPE (curve *e*), TR oxidation occurred at 0.6 V with a negative shift of 200 mV compared with 5ADMBCNPE. The peak current (I_p = 6.99 μA) at the nPt-5ADMBCNPE was 4.26 times that of the CPE and 1.45 times that of the nPt-CNPE. The remarkable enhancement of current response demonstrated that nPt-5ADMBCNPE acted as an efficient promoter to improve the electron transfer kinetics.

The effect of the potential scan rate (v) on the electrocatalytic property of nPt-5ADMBCNPE toward electrooxidation of LD and TR was studied by cyclic voltammetry (Fig. 5a). The peaks current increased with a positive shift in the potential when the scan rate increased (CV data for TR not shown), a typical characteristic of irreversible electrochemical reactions. A linear plot of the peak current ($I_{p,a}$) vs. the square root

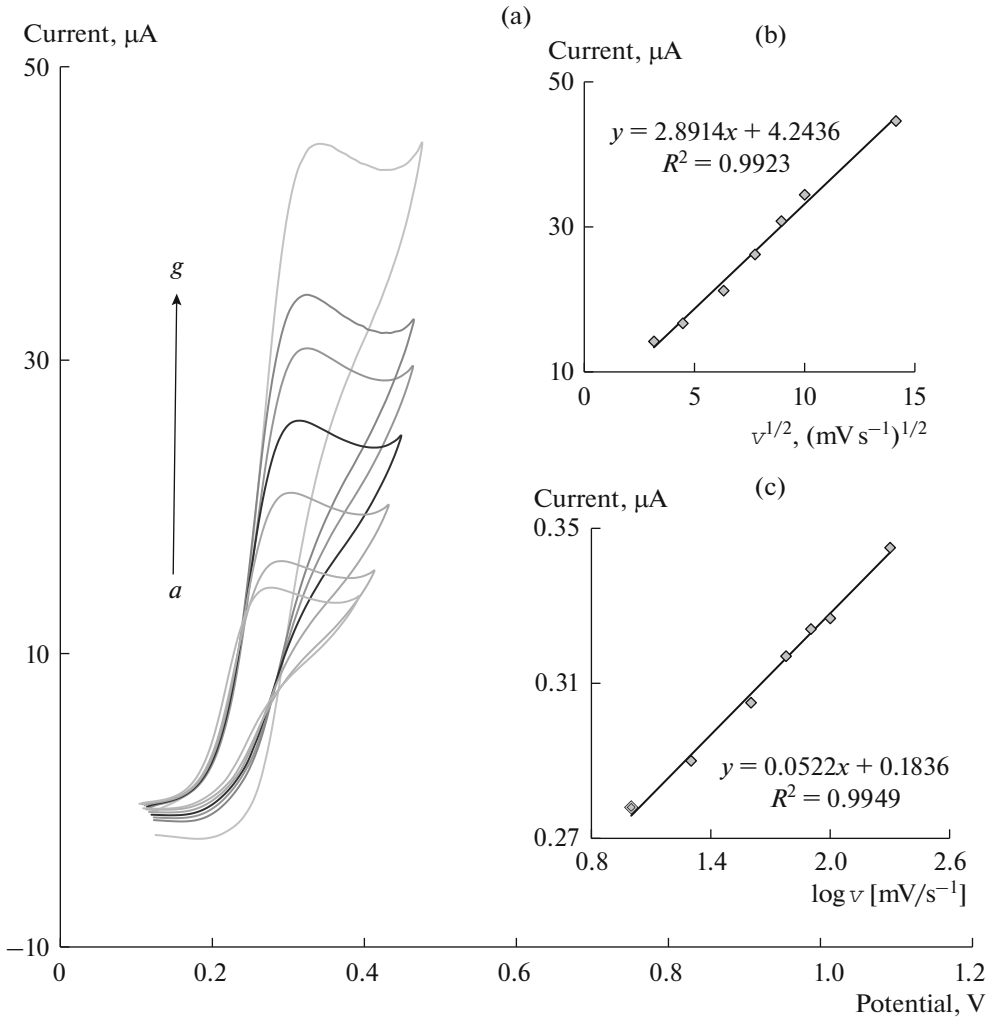

Fig. 5. (a) Cyclic voltammograms of 80.0 μM LD in 0.1 M PBS (pH 7.0) at nPt-5ADMBCNPE at various scan rates: (*a*) 10, (*b*) 20, (*c*) 40, (*d*) 60, (*e*) 80, (*f*) 100 and (*g*) 200 mV s^{-1}. (b) plot of $I_{p,a}$ vs. $v^{1/2}$ for 80.0 μM LD. (c) Dependence of the peak potential, on log *v* for the oxidation of LD at the nPt-5ADMBCNPE obtained from data of Fig. 5a.

of the scan rate ($v^{1/2}$) was obtained for both analytes, in the range from 0.01 to 0.20 V s^{-1} in a 0.1 M PBS (pH 7.0), confirming that the electrode process is controlled by diffusion (Fig. 5b).

In order to obtain information about the rate determining step, the Tafel slope (*b*), was determined using the following equation [38]:

$$E_p = (b/2)\log v + \text{constant}. \quad (1)$$

Base on Eq. (1), the slope of E_p versus log *v* plot is (*b*/2), where *b* indicates the Tafel slope. The slope of E_p versus log *v* plot was found to be 0.0522 and 0.0445 V for LD (Fig. 5c) and TR (data not shown) in this work, respectively. These slopes indicate a transfer coefficient (α) of 0.76 (for LD) and 0.67 (for TR) for a one electron transfer process, which is rate-determining step. The value of α is accordant to that reported in other works [39, 40]. These values clearly show that not only the over potential for LD oxidation is reduced at the surface of nPt-5ADMBCNPE, but also the rate of the electron transfer process is greatly enhanced. This phenomenon is thus confirmed by large $I_{p,a}$ values recorded during the cyclic voltammetry of 80.0 μM LD at nPt-5ADMBCNPE.

Chronoamperometric Studies

The catalytic oxidation of LD at the surface of the nPt-5ADMBCNPE was also investigated by chronoamperometry. Fig. 6a depicts the current vs. time curves of the modified electrode obtained by setting the working electrode potential at 0.32 V vs. Ag|AgCl|KCl (3.0 M) for various concentrations of LD in PBS (pH 7.0). The diffusion coefficient (D_{app}) for

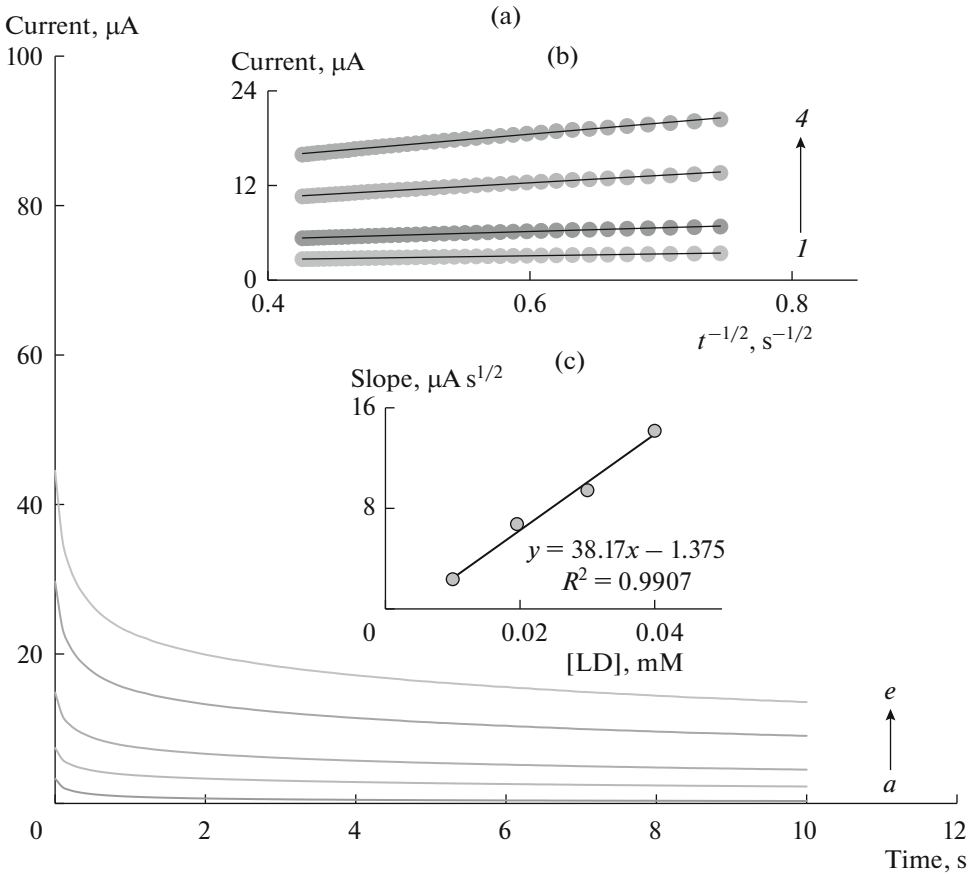

Fig. 6. (a) Chronoamperograms obtained at the nPt-5ADMBCNPE in the absence (*a*) and presence of (*b*) 0.01, (*c*) 0.02, (*d*) 0.03 and (*e*) 0.04 mM of LD in PBS (pH 7.0), potential step was 0.32 V vs. Ag|AgCl|KCl (3.0 M). (b) Plots of I vs. $t^{-1/2}$ obtained from chronoamperograms *b*–*e* in (a). (c) Plot of the slope of the straight lines against the LD concentration.

oxidation of LD at the surface of the modified electrode can be estimated using Cottrell's equation [38]:

$$I = nFAD_{app}^{1/2}c_b\pi^{-1/2}t^{-1/2},$$

where D_{app} and c_b, are the apparent diffusion coefficient ($cm^2\ s^{-1}$) and the bulk concentration ($mol\ cm^{-3}$), respectively. Under diffusion control conditions, the plot of I_p versus $t^{-1/2}$ would be linear, and the value of D_{app} could be estimated from the slope of this plot. Figure 6b shows the fitted experimental plots for different concentrations of LD in the range of 0.01–0.04 mM. The mean value of D_{app} was found to be 1.24×10^{-5} $cm^2\ s^{-1}$ using the slopes of the resulting straight lines plotted versus the LD concentrations (Fig. 6c).

Calibration Plot and Limit of Detection

Since, differential pulse voltammetry (DPV) has the advantage of an increase in sensitivity and better characteristics for analytical applications, therefore, differential pulse voltammetry experiments were performed using nPt-5ADMBCNPE in phosphate buffer solution containing various concentrations of LD and TR. The plot of peak current vs. LD and TR concentration consisted of a linear range with slopes of 0.1116 and 0.1042 A M^{-1} in the concentration ranges of 0.50–100.0 μM and 0.60–100.0 μM, respectively (data not shown). The detection limit defined as $3S_b/m$ (where S_b is the standard deviation of the blank signal ($n = 6$) and m is the slope of the calibration curve) for determination of LD and TR were found to be 0.31 and 0.52 μM, respectively. As expected, a very low LOD at the nPt-5ADMBCNPE was obtained, which can be attributed to the presence of MWCNTs and Pt nanoparticles in structure of modified electrode.

Simultaneous Determination of LD and TR

The main objective of this study was to measure LD and TR simultaneously. For this purpose, the effective application of the nPt-5ADMBCNPE for electrooxidation processes of LD and TR in the mixture was investigated when the concentration of one species changed while the other species was kept constant.

The results are shown in Figs. 7a, 7b. As it can be seen, the peak current of LD increased with an increase in LD concentration when the concentration of TR was kept constant (Fig. 7a). Similarly and obviously, as shown in Fig. 7b, keeping the concentration of LD constant, the oxidation peak current of TR was positively proportional to its concentration. The obtained DPV response with two well-distinguished anodic peaks, corresponding to the oxidation of LD and TR, is indicating that the simultaneous determination of LD and TR is possible at the nPt-5ADMBCNPE.

Interference Study

The influence of various foreign species on the determination of 10^{-4} M LD and 6.0×10^{-5} M TR was investigated. The tolerance limit was taken as the maximum concentration of the foreign substances, which caused an approximately ±5% relative error in the determination. The tolerated concentration of foreign substances was 1.0×10^{-1} M for Na^+, Cl^-, F^-, S^{2-}, CO_3^{2-}, HCO^{3-}, NO_3^{2-}, and K^+; 5.0×10^{-2} M for Mg^{2+}, Cd^{2+}, Ba^{2+}, Ni^{2+}, Al^{3+},Cu^{2+}, Pb^{2+} and Ca^{2+}; 4.0×10^{-3} M for *l*-lysine, glucose, lactose, fructose, sucrose, *l*-asparagines, glutamic acid, glycine, *l*-cystine, acetaminophen, riboflavin and NADH.

However, investigation about all of interfering components is impossible. The studied interferences are the common interfering agents at the real samples [41–43]. The phosphates cannot be interfering materials because of the all of experiments were done at the phosphate buffer solutions. On the other hand, the urine sample was used without any specific sample pretreatment such as solid phase extraction and no interference of the matrix components was observed. Therefore, it was not necessary to investigate all of probably interfering agents such as nitrogen-containing decomposition products of proteins when analyzing human urine samples. Also, ascorbic acid, dopamine, epinephrine and norepinephrine showed interference on determination of LD.

Sample Analysis Individual Determination of LD and TR in Pharmaceutical Samples and Dairy Products

Five tablets of LD were weighed and ground. An adequate amount of the obtained fine powder, equivalent to a stock solution of concentration about 0.01 M, dissolved in 0.1 M phosphate buffer pH 7.0 using an ultrasonic bath for 4 min. Different amounts of this solution, covering the working concentration range of 0.50–100.0 μM, were transferred into the 10.0 mL voltammetric cell and analyzed by standard addition method. The obtained results for two commercialized pharmaceutical formulations are given in Table 1. Also, applicability of the nPt-5ADMBCNPE for real-life sample analysis was used for the determi-

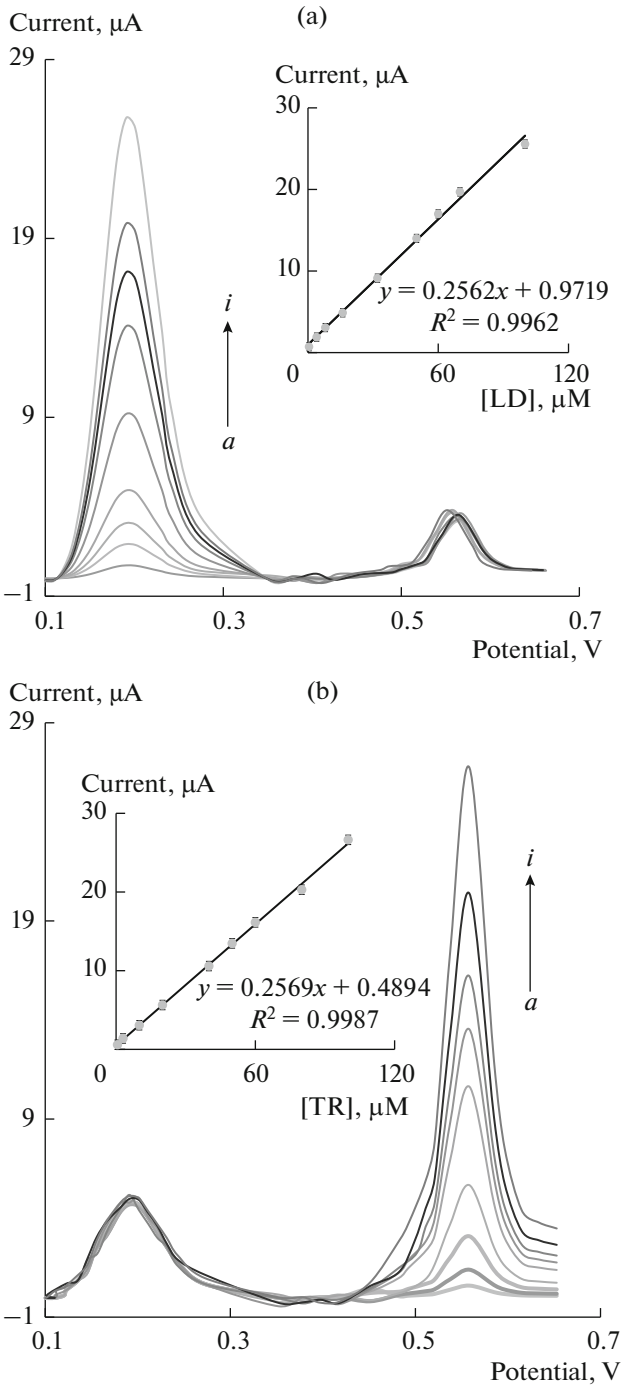

Fig. 7. (a) DPV signals for solutions containing of TR (5.0 μM) and different concentrations of LD: (*a*) 0.5, (*b*) 4.0, (*c*) 8.0, (*d*) 16.0, (*e*) 32.0, (*f*) 50.0, (*g*) 60.0, (*h*) 70.0 and (*i*) 100.0 μM in 0.1 M PBS (pH 7.0) at the nPt-5ADMBCNPE. Inset: Calibration plot of peak current vs. LD concentration. (b) DPVs for solutions containing of LD (20.0 μM) and different concentrations of TR: (*a*) 0.6, (*b*) 3.0, (*c*) 10.0, (*d*) 20.0, (*e*) 40.0, (*f*) 50.0, (*g*) 60.0, (*h*) 80.0 and (*i*) 100.0 μM in 0.1 M PBS (pH 7.0) at the nPt-5ADMBCNPE. Inset: Calibration plot of peak current vs. TR concentration.

Table 1. Determination of LD and TR in pharmaceutical samples and dairy products ($n = 5$) at nPt-5ADMBCNPE

Sample	LD[a]		TR[b]	
Added, μM	20.00	30.00	10.00	40.00
Found, μM	20.60	29.86	10.12	40.76
Recovery, %	103	99.53	101.2	101.9
RSD, %	±1.8	±1.6	±1.4	±1.9
Labelledclaim, mg	110	250	–	–
Mean amount found, mg	113.3	248.8	–	–

[a] Ramopharmin Pharmaceutical Co., Tehran, Iran.
[b] Yoghurt (kefir) sample KallehAmol Co., Amol, Iran.

Table 2. Voltammetric determination of LD and TR in urine samples ($n = 5$) at nPt-5ADMBCNPE

Sample	LD added, μM	LD found, μM	Recovery, %	TR added, μM	TR found, μM	Recovery, %
1	6.0	6.12 (±0.02)	102	5.0	5.4 (±0.02)	108.0
2	20.0	20.56 (±0.01)	102.8	30.0	30.8 (±0.01)	102.6
3	80.0	80.16 (±0.02)	100.2	60.0	60.17 (±0.01)	100.2

nation of TR in yoghurt (kefir) samples. For this purpose 10.0 mL yoghurt samples (Kalleh Amol Co., Amol, Iran) with certain amount of standard solutions of TR, at working concentration range of 0.60–100.0 μM, was added into voltammetric cell and analyzed by the same procedure. To evaluate the accuracy of this method in the voltammetric determination of TR, the percentage recovery values for the samples are shown in Table 1.

Application of nPt-5ADMBCNPE for Simultaneous Determination of LD and TR in Real Samples

One of the main objectives of sensors is their capability in distinguishing related analytes in real samples. Hence, the applicability of the nPt-5ADMBCNPE was investigated for detection of LD and TR in urine samples. The standard addition method was used for the determination of LD and TR using DPV method. Satisfactory recovery of the experimental results was found for LD and TR. Also, the efficiency of this modified electrode was credible for voltammetric determination of these three compounds in same solution. The results are shown in Table 2.

CONCLUSIONS

This work demonstrates the construction of an nPt-5ADMBCNPE and its application in simultaneous determination of LD and TR. The results showed two well-defined redox peaks for oxidation of LD and TR at the surface of the nPt-5ADMBCNPE, which were large enough to determine LD and TR individually and in presence of each other. The low-cost, simplicity and fast construction of the sensor make it superior to other techniques for simultaneous determination of LD and TR. Satisfactory results were obtained using these sensors in real sample analysis.

REFERENCES

1. Hernández-Cázares, A.S., Aristoy, M.C., and Toldrá, F., *J. Food Eng.*, 2011, vol. 110, p. 324.
2. Bulushi, I.A., Poole, S., Deeth, H.C., and Dykes, G.A., *Crit. Rev. Food Sci. Nutr.*, 2009, vol. 49, p. 369.
3. Önal, A., *Food Chem.*, 2007, vol. 103, p. 1475.
4. Lovenberg, W., *Some vaso- and psychoactive substances in food, toxicants occurring naturally in foods*, 2nd ed., *Natl. Acad. Sci.*, Washington DC, 1973.
5. Masson, F., Talon, R., and Montel, M.C., *Int. J. Food Microbiol.*, 1996, vol. 32, p. 199.
6. Santos-Buelga, C., Nogales-Alarcon, A., and Marine-Font, A., *J. Food Sci.*, 1981, vol. 46, p. 1794.
7. Lapainis, T., Scanlan, C., Rubakhin, S.S., and Sweedler, J.V., *Anal. Bioanal. Chem.*, 2007, vol. 387, p. 97.
8. Ladero, V., Martínez, N., Martín, M.C., Fernández, M., and Alvarez, M.A., *Food Res. Int.*, 2010, vol. 43, p. 289.
9. Huang, K.J., Wei, C.Y., Liu, W.L., Xie, W.Z., Zhang, J.F., and Wang, W., *J. Chromatogr. A*, 2009, vol. 1216, p. 6636.
10. Banks, C.N. and Adams, M.E., *Toxicon*, 2012, vol. 59, p. 320.
11. Mazloum-Ardakani, M., Beitollahi, H., Ganjipour, B., Naeimi, H., and Nejati, M., *Bioelectrochemistry*, 2009, vol. 75, p. 1.
12. Huang, J., Xing, X., Zhang, X., He, X., Lin, Q., Lian, W., and Zhu, H., *Food Res. Int.*, 2011, vol. 44, p. 276.
13. Daneshgar, P., Norouzi, P., Ganjali, M.R., Ordikhani-Seyedlar, A., and Eshraghi, H., *Colloid. Surf. B*, 2009, vol. 68, p. 27.

14. Tolokan, A., Klebovich, I., Balogh-Nemes, K., and Horvai, G., *J. Chromatogr. B*, 1997, vol. 698, p. 201.
15. Zhao, S., Bai, W., Wang, B., and He, M., *Talanta*, 2007, vol. 73, p. 142.
16. Teixeira, M.F., Bergamini, M.F., Marques, C.M., and Bocchi, N., *Talanta*, 2004, vol. 63, p. 1083.
17. Shahrokhian, S. and Asadian, E., *J. Electroanal. Chem.*, 2009, vol. 636, p. 40.
18. Stockley, I.H., *Monoamine Oxidase Inhibitor Drug Interactions*, Oxford, U.K.: Drug Interactions, Blackwell Scientific Publications, 1993.
19. Lin, J. and Cashman, J.R., *Chem. Res. Toxicol.*, 1997, vol. 10, p. 842.
20. Marley, E., Blackwell, B., and Histamine, D., *Adv. Pharmacol. Chemother.*, 1971, vol. 8, p. 185.
21. Merino, M., Nuñez-Vergara, L.J., and Squella, J.A., *Electroanalysis*, 1999, vol. 11, p. 1285.
22. Beitollahi, H. and Mostafavi, M., *Electroanalysis*, 2014, vol. 26, p. 1090.
23. Mahmoudi Moghaddam, H., Beitollahi, H., Tajik, S., and Soltani, H., *Electroanalysis*, 2015, vol. 27, p. 2620.
24. Beitollahi, H. and Nekooei, S., *Electroanalysis*, 2015, vol. 28, p. 645.
25. Jahani, S. and Beitollahi, H., *Electroanalysis*, 2016, vol. 28, no. 9, p. 2022. doi 10.1002/elan.201501136
26. Molaakbari, E., Mostafavi, A., Beitollahi, H., and Alizadeh, R., *Analyst*, 2014, vol. 139, p. 4356.
27. Beitollahi, H., Karimi-Maleh, H., and Khabazzadeh, H., *Anal. Chem.*, 2008, vol. 80, p. 9848.
28. Beitollahi, H., Gholami, A., and Ganjali, M.R., *Mat. Sci. Eng. C*, 2015, vol. 57, p. 107.
29. Baghayeri, M., Amiri, A., and Farhadi, S., *Sens. Actuat. B*, 2016, vol. 225, p. 354.
30. Yoon, J.H., Muthuraman, G., Yang, J., Shim, Y.B., and Won, M. S., *Electroanalysis*, 2007, vol. 19, p. 1160.
31. Karam, P., Xin, Y., Jaber, S., and Halaoui, L.I., *J. Phys. Chem. C*, 2008, vol. 112, p. 13846.
32. Zheng, S.F., Hu, J.S., Zhong, L.S., Wan, L.J., and Song, W.G., *J. Phys. Chem. C*, 2007, vol. 111, p. 11174.
33. Raoof, J.B., Baghayeri, M., and Ojani, R., *Colloid. Surf. B*, 2012, vol. 95, p. 121.
34. Beitollahi, H., Ardakani, M.M., Ganjipour, B., and Naeimi, H., *Biosens. Bioelectron.*, 2008, vol. 24, p. 362.
35. Mazloum-Ardakani, M., Ganjipour, B., Beitollahi, H., Amini, M.K., Mirkhalaf, F., Naeimi, H., and Nejati-Barzoki, M., *Electrochim. Acta*, 2011, vol. 56, p. 9113.
36. Laviron, E., *J. Electroanal. Chem.*, 1974, vol. 52, p. 355.
37. Beitollahi, H., Mohadesi, A., Mahani, S.K., and Akbari, A., *Anal. Methods*, 2012, vol. 4, p. 1029.
38. Pournaghi-Azar, M.H. and Razmi-Nerbin, H., *J. Electroanal. Chem.*, 2000, vol. 488, p. 17.
39. Raoof, J.B., Ojani, R., Amiri-Aref, M., and Baghayeri, M., *Sens. Actuat. B*, 2012, vol. 166, p. 508.
40. Raoof, J.B., Ojani, R., Baghayeri, M., and Amiri-Aref, M., *Anal. Methods*, 2012, vol. 4, p. 1579.
41. Goyal, R.N., Gupta, V.K., and Bachheti, N., *Anal. Chim. Acta*, 2007, vol. 597, p. 82.
42. Sanghavi, B.J. and Srivastava, A.K., *Analyst*, 2013, vol. 138, p. 1395.
43. Atta, N.F., El-Kady, M.F., and Galal, A., *Anal. Biochem.*, 2010, vol. 400, p. 78.